

# ***RTD Class-AA Replacement With High-Accuracy Digital Temperature Sensors in Field Transmitters***

Amit Ashara

## **ABSTRACT**

Field transmitters are used extensively in factory automation and control-to-sense process parameters like temperature, pressure, and flow rate, to name a few. This information is then relayed to a programmable logic controller (PLC) to make real time decisions that impact the efficiency and reliability of an industrial system. The sensors used in the field transmitters are mostly analog sensors that must be sampled accurately using an analog front-end (AFE). Due to the operational conditions that arise from the placement of the field transmitters, it may be subjected to wide varying temperature conditions and hence, require some form of temperature compensation. Traditionally, accurate temperature sensors like Class-AA resistance temperature detector (RTD) are used in such temperature compensation systems.

Texas Instruments now offers the TMP117, which is a high-accuracy and low-power integrated temperature sensor, that can effectively replace Class-AA RTD in a host of field transmitter applications. This application note intends to serve as a comprehensive design guideline for customers looking for precision sensing with field transmitters, while drastically reducing the overall system complexity, development time, and cost when compared to an RTD.

## **Contents**

1	Introduction .....	2
2	System Description .....	3
3	Related Designs .....	19
4	Summary .....	20
5	References .....	20

## **List of Figures**

1	Temperature Transmitter Block Diagram .....	2
2	2-Wire RTD Circuit .....	4
3	3-Wire RTD Circuit .....	5
4	4-Wire RTD Circuit .....	6
5	Accuracy Chart for TMP117 and RTD .....	7
6	3-Wire Ratiometric RTD Circuit .....	9
7	Current Source Mismatch Compensation for RTD .....	10
8	TMP117 Block Diagram for CJC .....	11
9	RTD Top Layer Placement .....	12
10	RTD Internal Layer Placement .....	13
11	RTD Bottom Layer Placement .....	14
12	TMP117 Placement .....	15
13	TMP117 3D Placement View .....	16
14	RTD Software Time Graph .....	18
15	TMP117 Software Time Graph .....	19
16	TIDA-010019 Block Diagram .....	20

## **List of Tables**

1	Constant Value per Standards .....	3
2	RTD Accuracy by Class and Type .....	3
3	TMP117 Accuracy Specification .....	7
4	ADC Specification and Parameters .....	16

**Trademarks**

SMBus is a trademark of Intel Corporation.  
 All other trademarks are the property of their respective owners.

**1 Introduction**

A field transmitter is a device that can convert the signal produced by a sensor into an instrumentation signal which can then be transmitted to an indicating or controlling device. The field transmitter often combines both the sensor and the transmitter in a single system. Figure 1 shows the block diagram for a temperature transmitter for a thermocouple with Cold Junction Compensation (CJC). As can be seen in the block diagram, a typical signal chain has an AFE that can convert the analog signal from a sensor to a digital signal. The signal can be processed by a microcontroller (MCU), and the data can be transmitted wirelessly or over a wired bus depending on the system requirements.

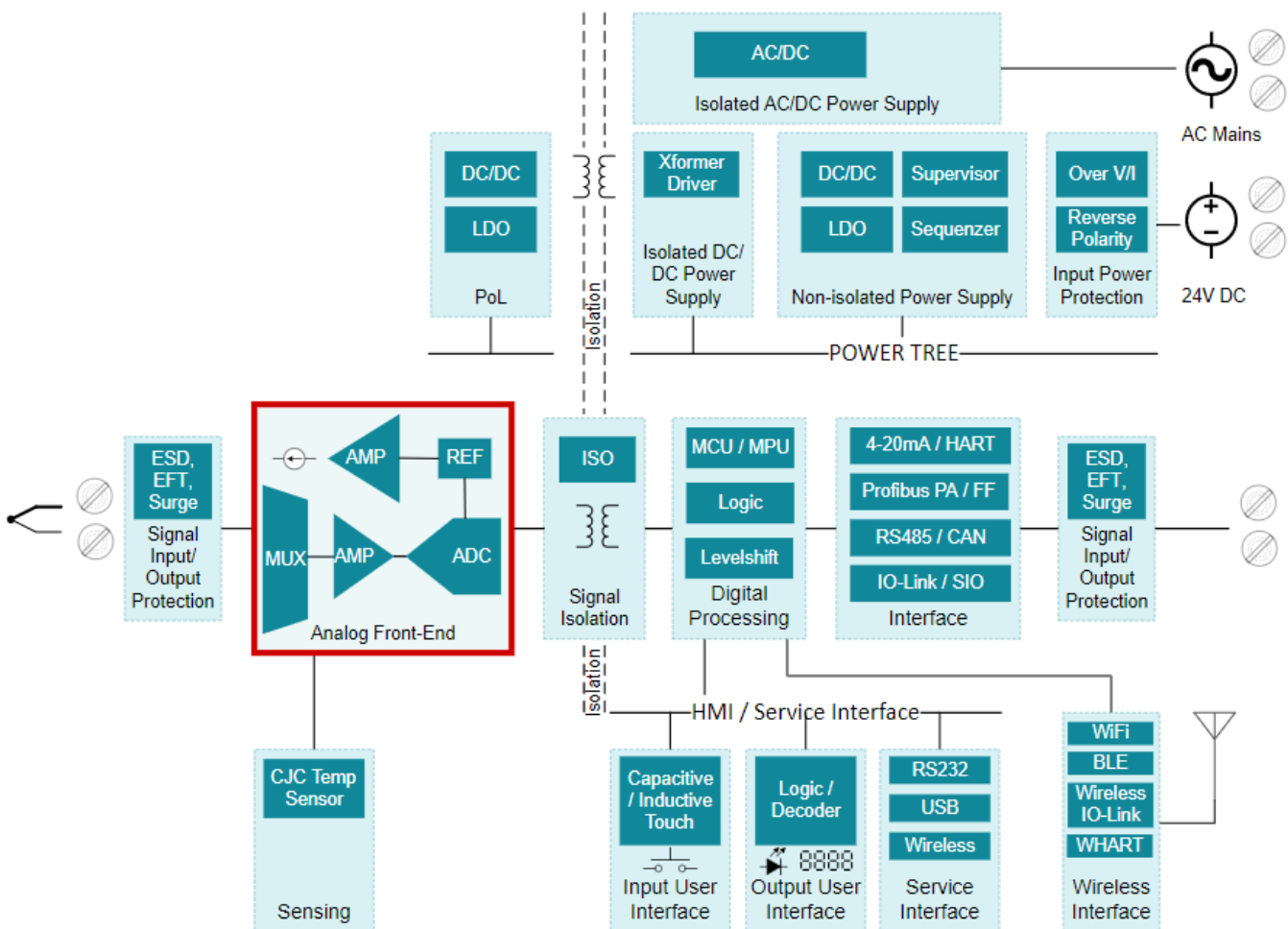


**Figure 1. Temperature Transmitter Block Diagram**

## 2 System Description

One of the most common uses for high-accuracy RTDs is in temperature transmitters where RTDs are used as the main precision element for cold junction compensation (CJC). The following sections will briefly describe a typical temperature transmitter with an RTD as the CJC element. Also, while the RTD can conceptually be treated as a sensor, the designer must carefully consider which components to use and where to place them to achieve a high degree of precision for temperature compensation. [Equation 1](#) shows a simplified version of the resistance equation.

$$R_T = R_0 \times (1 + A \times T + B \times T^2 + C \times T^3 \times (T - 100))$$

where

- $R_T$  is the resistance at temperature  $T^\circ\text{C}$
- $R_0$  is the nominal resistance at  $0^\circ\text{C}$
- A, B and C are constants used to scale the RTD.

(1)

**Table 1. Constant Value per Standards**

Standard	Temperature Coefficient ( $\alpha$ )	A	B	C*
DIN 43760	0.003850 $\Omega/\Omega^\circ\text{C}$	$3.908 \times 10^{-3}$	$-5.8019 \times 10^{-7}$	$-4.2735 \times 10^{-12}$
American	0.003911 $\Omega/\Omega^\circ\text{C}$	$3.9692 \times 10^{-3}$	$-5.8495 \times 10^{-7}$	$-4.2325 \times 10^{-12}$
ITS-90	0.003926 $\Omega/\Omega^\circ\text{C}$	$3.9848 \times 10^{-3}$	$-5.870 \times 10^{-7}$	$-4.0000 \times 10^{-12}$

**NOTE:** This is for temperature below  $0^\circ\text{C}$  only; C = 0.0 for temperatures above  $0^\circ\text{C}$ .

### 2.1 RTD Description

An RTD most commonly consists of a thin gauge pure metal platinum wire wound on a ceramic housing (wire-wound) or in the form of a metal-coated substrate (film-type). [Table 2](#) shows the accuracy for different RTD type by class. RTD typically are 100- $\Omega$  platinum type, but can also be in a 500- $\Omega$  or 1000- $\Omega$  type. The basic theory of operation for an RTD is based on the change of resistance of the platinum wire with temperature. This temperature coefficient of resistance is characterized by the parameter  $\alpha$ ; and is the linear approximation of the resistance versus temperature between  $0^\circ\text{C}$  and  $100^\circ\text{C}$ .

**Table 2. RTD Accuracy by Class and Type**

RTD Class	Wire-Wound Temperature Range	Thin-Film Temperature Range	Tolerance Value ( $^\circ\text{C}$ )	Resistance at $0^\circ\text{C}$ ( $\Omega$ )	Error at $100^\circ\text{C}$ ( $\Omega$ )	Error Over Wire-Wound Range ( $^\circ\text{C}$ )
AA	$-50^\circ\text{C}$ to $+250^\circ\text{C}$	$0^\circ\text{C}$ to $+150^\circ\text{C}$	$\pm(0.1 + 0.0017 \times T)$	$100 \pm 0.04$	0.27	0.525
A	$-100^\circ\text{C}$ to $+450^\circ\text{C}$	$-30^\circ\text{C}$ to $+300^\circ\text{C}$	$\pm(0.15 + 0.002 \times T)$	$100 \pm 0.06$	0.35	1.05
B	$-196^\circ\text{C}$ to $+600^\circ\text{C}$	$-50^\circ\text{C}$ to $+500^\circ\text{C}$	$\pm(0.3 + 0.005 \times T)$	$100 \pm 0.12$	0.8	3.3
C	$-196^\circ\text{C}$ to $+600^\circ\text{C}$	$-50^\circ\text{C}$ to $+600^\circ\text{C}$	$\pm(0.6 + 0.01 \times T)$	$100 \pm 0.24$	1.6	6.6

An RTD construction topology may be a 2-wire, 3-wire, or 4-wire type described in the following sections.

### 2.1.1 2-Wire RTD

Figure 2 shows a 2-wire construction for an RTD. It is the least accurate construction and is used mostly when there are short lead wires or when accuracy is not a consideration, as the resistance of the lead wires also add to the measured resistance.

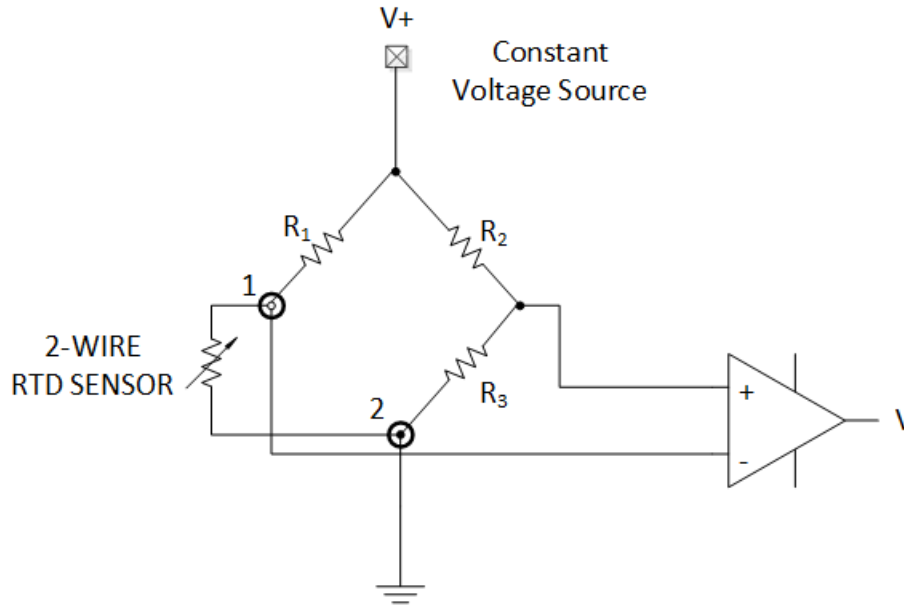
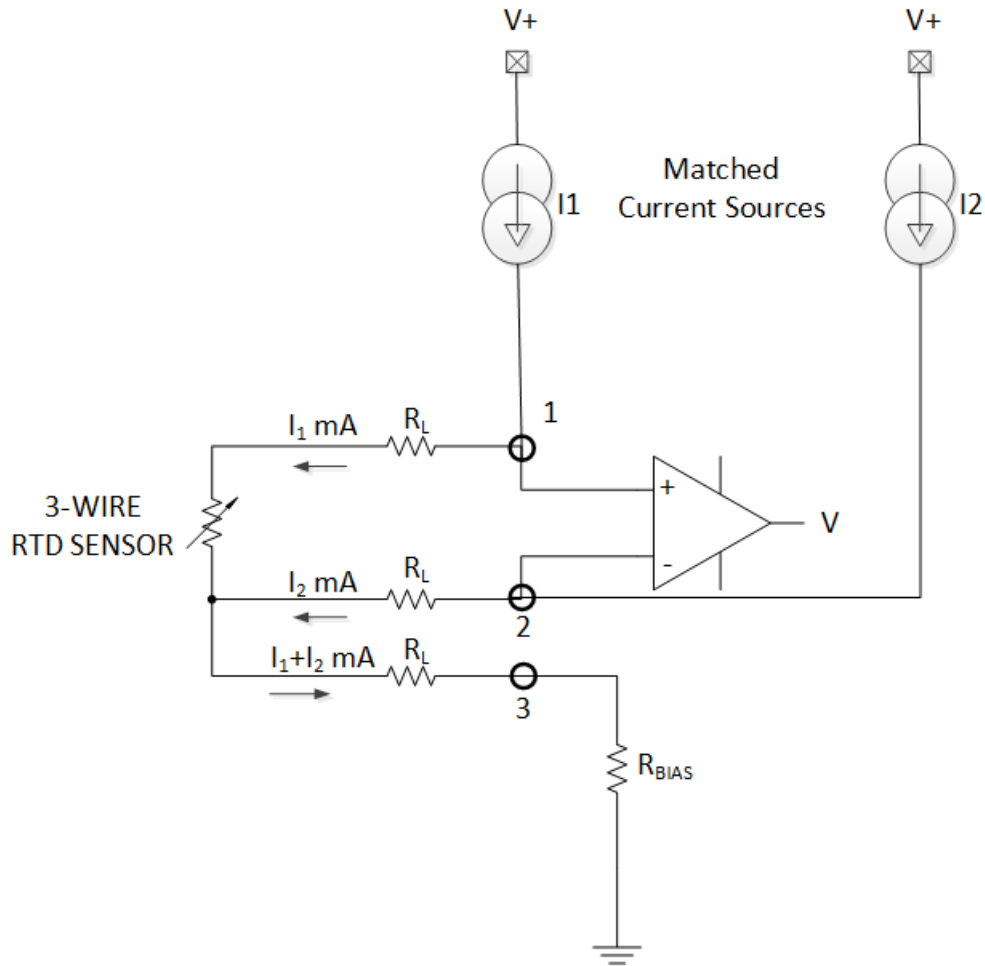


Figure 2. 2-Wire RTD Circuit

**2.1.2 3-Wire RTD**

Figure 3 shows a 3-wire construction for an RTD. It is the most commonly used construction in industrial application. The third wire provides a method for removing the average lead wire resistance from the sensor measurement.



**Figure 3. 3-Wire RTD Circuit**

### 2.1.3 4-Wire RTD

Figure 4 shows a 4-wire construction for an RTD. In this construction, the actual resistance of the lead wires can be determined and removed from the sensor measurement. The current flows between leads 1 and 4, and the voltage sensing is done between leads 2 and 3. Almost no current flows in leads 2 and 3, therefore the measurement of the voltage across the sense element is very accurate. If there is some distance involved, however, this method is expensive.

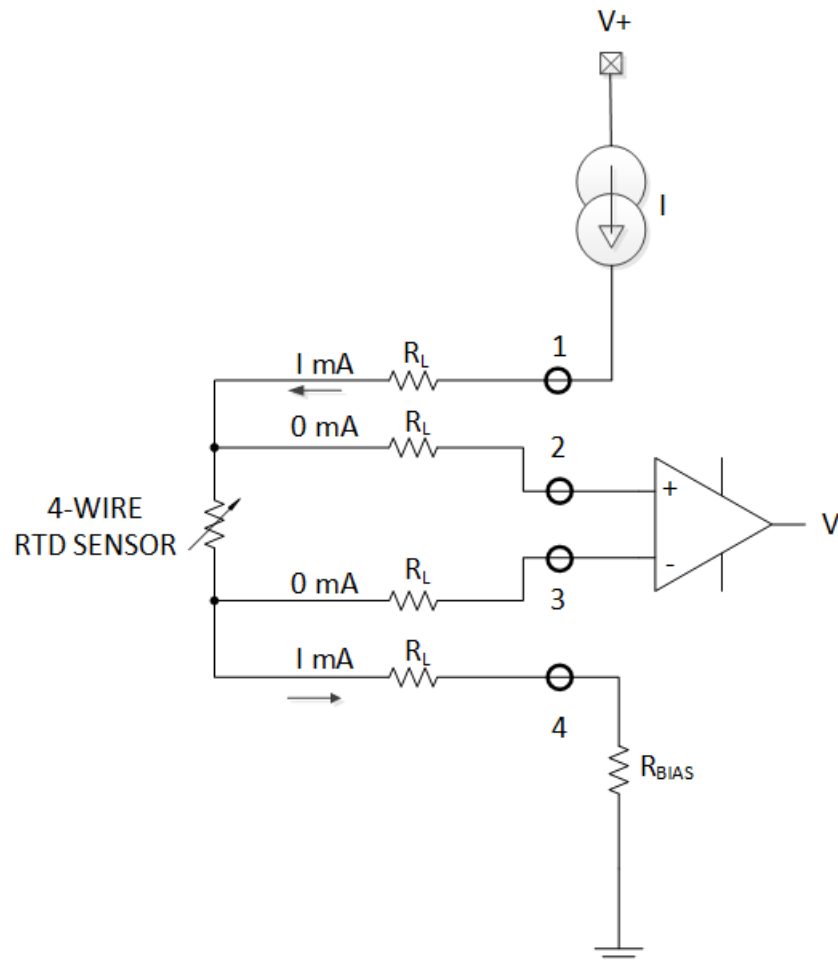


Figure 4. 4-Wire RTD Circuit

## 2.2 TMP117 Description

The TMP117 is a high-precision digital temperature sensor which provides a 16-bit result with a resolution of 0.0078°C and an accuracy of up to  $\pm 0.1^\circ\text{C}$  across the  $-20^\circ\text{C}$  to  $+50^\circ\text{C}$  temperature range with no calibration. The TMP117 is I<sup>2</sup>C- and SMBus™ interface compatible, has a programmable alert function, and can allow up to four devices on a single bus. The overall accuracy of the TMP117 across its operating range is given in [Table 3](#).

**Table 3. TMP117 Accuracy Specification**

Temperature Range	Accuracy
$-20^\circ\text{C}$ to $+50^\circ\text{C}$	$\pm 0.1^\circ\text{C}$
$-40^\circ\text{C}$ to $+100^\circ\text{C}$	$\pm 0.2^\circ\text{C}$
$-55^\circ\text{C}$ to $+150^\circ\text{C}$	$\pm 0.3^\circ\text{C}$

The accuracy of the TMP117 versus an RTD is plotted in [Figure 5](#) across the operating temperature range of  $-55^\circ\text{C}$  to  $+150^\circ\text{C}$ . It is evident looking at the [Figure 5](#) that the TMP117 with no calibration has the same or better accuracy as an RTD Class-AA sensor. Note that this is the raw accuracy of the two devices and that the final system layout has a minor effect on the TMP117 and a major effect on the accuracy of an RTD sensor due to a number of parameters like the choice of ADC, layout of signal traces, component tolerances, and so forth. For further details on how to calculate the system level accuracy of an RTD sensor, refer to . As can be seen in the reference article, the extensive calibration required for an RTD system implementation is not necessary for the TMP117.

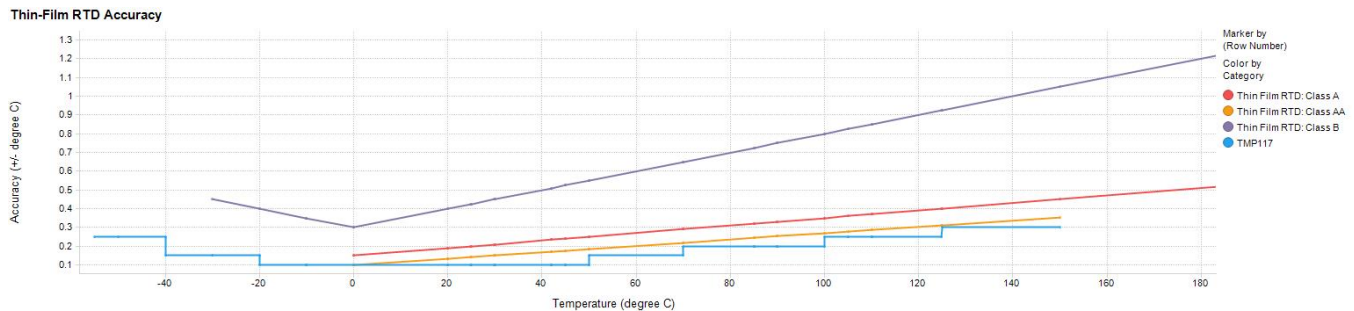


**Figure 5. Accuracy Chart for TMP117 and RTD**

### 2.3 Thermocouple Temperature Transmitter With CJC

Having gone through some basics on RTD, this section will elaborate on temperature transmitters that use RTD for CJC. Temperature transmitters commonly use thermocouples because they can withstand temperature extremes. A thermocouple consists of two dissimilar metals joined together to form two junctions. The voltage generated by this construction is a function of the temperature difference between the two junctions and is referred to as the Seebeck effect. The sensing junction is commonly referred to as the hot junction, while the measuring or reference junction is referred to as the cold junction. The cold junction consists of a third metal like copper, therefore, the temperature must be accurately known for the cold junction to determine the actual temperature at the hot junction.

An RTD in 3-wire construction is commonly used to measure the cold junction temperature due to its accuracy and repeatability of the measurements. Other temperature-sensing elements like thermistors may be used, but this requires a substantial amount of software for the linearization of the curve, and accuracy may be a problem. An RTD as the CJC element, requires special circuit handling to make sure that the accuracy can be maintained. A very common yet effective circuit for RTD uses a ratiometric measurement as shown in [Figure 6](#).

As can be seen in the representative circuit diagram, the system requires a precision ADC with current source muxing and high resolution. Even though the reference voltage is generated using the same current source, the temperature tolerances of the resistor need to be stringent to avoid a large change in the reference voltage due to temperature drift caused by the resistor. Thus, the cost of the three crucial components, namely the RTD, the ADC, and the reference resistor, is much higher due to the system performance requirement.

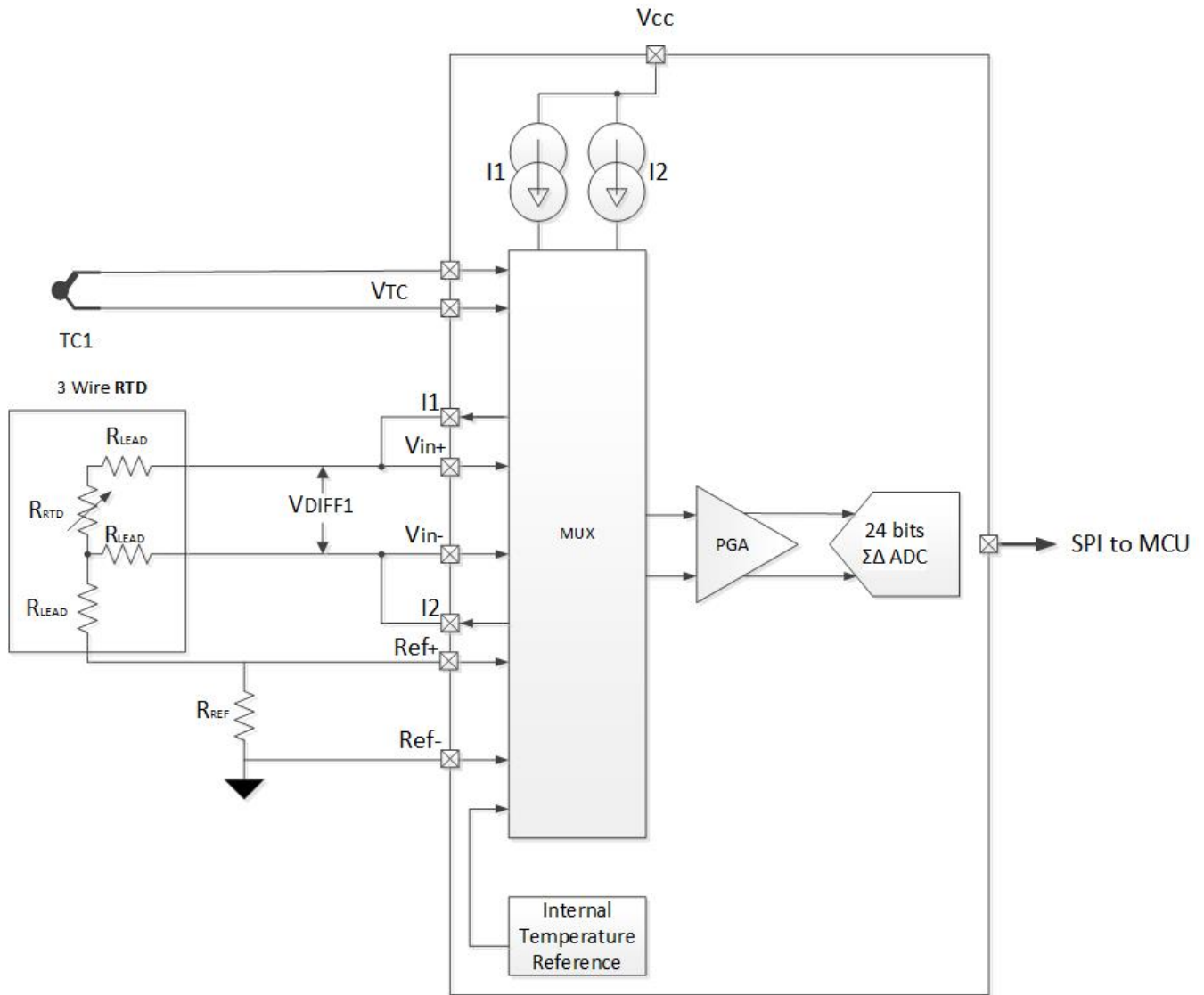
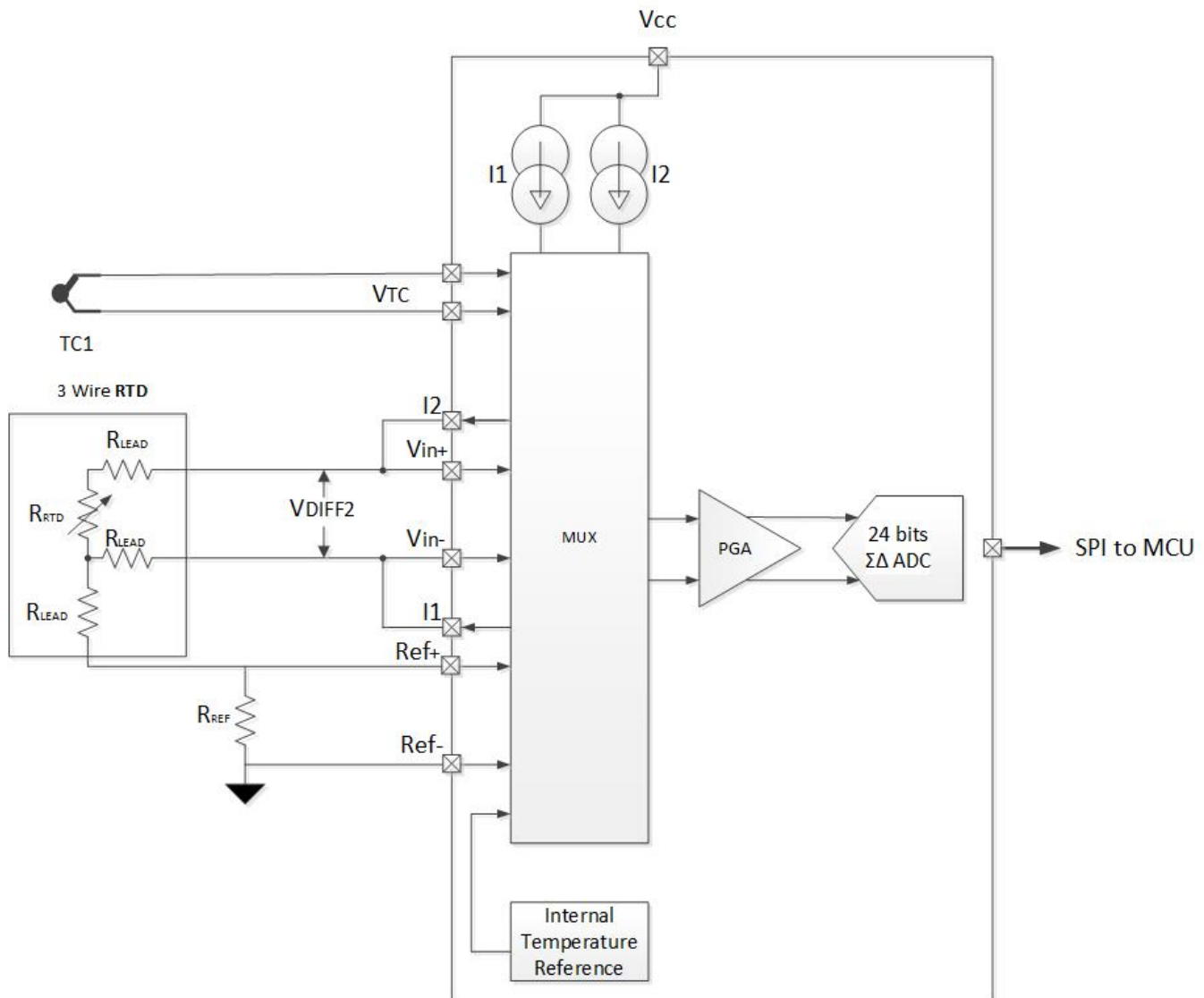


Figure 6. 3-Wire Ratiometric RTD Circuit

### 2.3.1 CJC Circuit Analysis for RTD

As shown earlier in Figure 6, for measuring the cold junction temperature with a 3-wire RTD, currents  $I_1$  and  $I_2$  are sourced by the ADC into the leads 1 and 2 of the RTD. This results in the voltage difference,  $V_{DIFF1}$ , that is generated across the leads and then sampled by the ADC. The sum of the currents  $I_1$  and  $I_2$  is used to generate a reference voltage across the reference resistor  $R_{REF}$ . Ideally, the two currents should match. Like in any real system, however, there is a certain amount of mismatch.

To compensate for the mismatch, the current sources are then swapped so that current  $I_1$  and  $I_2$  are now sourced by the ADC into leads 2 and 1 (as shown in Figure 7). As the sum of the current does not change, the reference voltage generated across  $R_{REF}$  remains the same. On conversion, the  $V_{DIFF2}$  voltage sensed by the ADC causes the mismatch to be effectively eliminated when the  $V_{DIFF2}$  is averaged with the  $V_{DIFF1}$ .



**Figure 7. Current Source Mismatch Compensation for RTD**

The effective  $V_{DIFF}$  can now be converted to a temperature using Equation 1, or by means of a look-up table in a MCU. While this seems very effective, the MCU has to perform two conversions to get an accurate temperature measurement. This is one of the most crucial steps in temperature measurement for the cold junction.

The ADC that is used for such a conversion would require to be a specialized ADC to allow muxing the current source that may not be a low-cost ADC. Also, the reference resistor that used  $R_{REF}$  must be a precision resistor with a tolerance of 0.1% or better so that the temperature change at the cold junction does not cause the reference voltage to shift. This is not a trivial cost increase for the system due to requirements for specialized components.

### 2.3.2 CJC Circuit Analysis With TMP117

The circuit for CJC can be incredibly simplified using the TMP117 high-precision digital temperature sensor. Figure 8 shows a typical block diagram for the application of TMP117 in CJC. The external components required to sense the temperature with the TMP117 is limited to a minimum of two pullup resistors for the I<sup>2</sup>C-interface and one decoupling capacitor. At the same time, these components do not require high tolerances, which drastically decreases the cost of the system implementation. Also the large number of components for the temperature compensation circuit with RTD is no longer required and a simpler but precise ADC can be used for sensing the thermocouple.

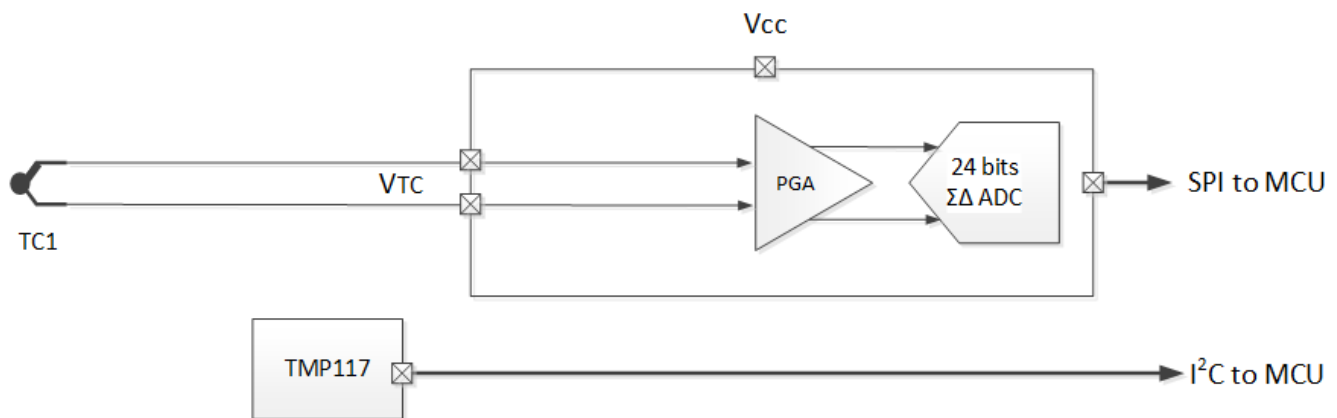


Figure 8. TMP117 Block Diagram for CJC

### 2.3.3 Component Placement Analysis

The following images show the placement and routing of a high-precision sigma-delta ADC along an RTD-based CJC design. For reference, the isothermal block shown is approximately 740 mils wide.

---

**NOTE:** One mil is equal to one-thousandth of an inch.

---

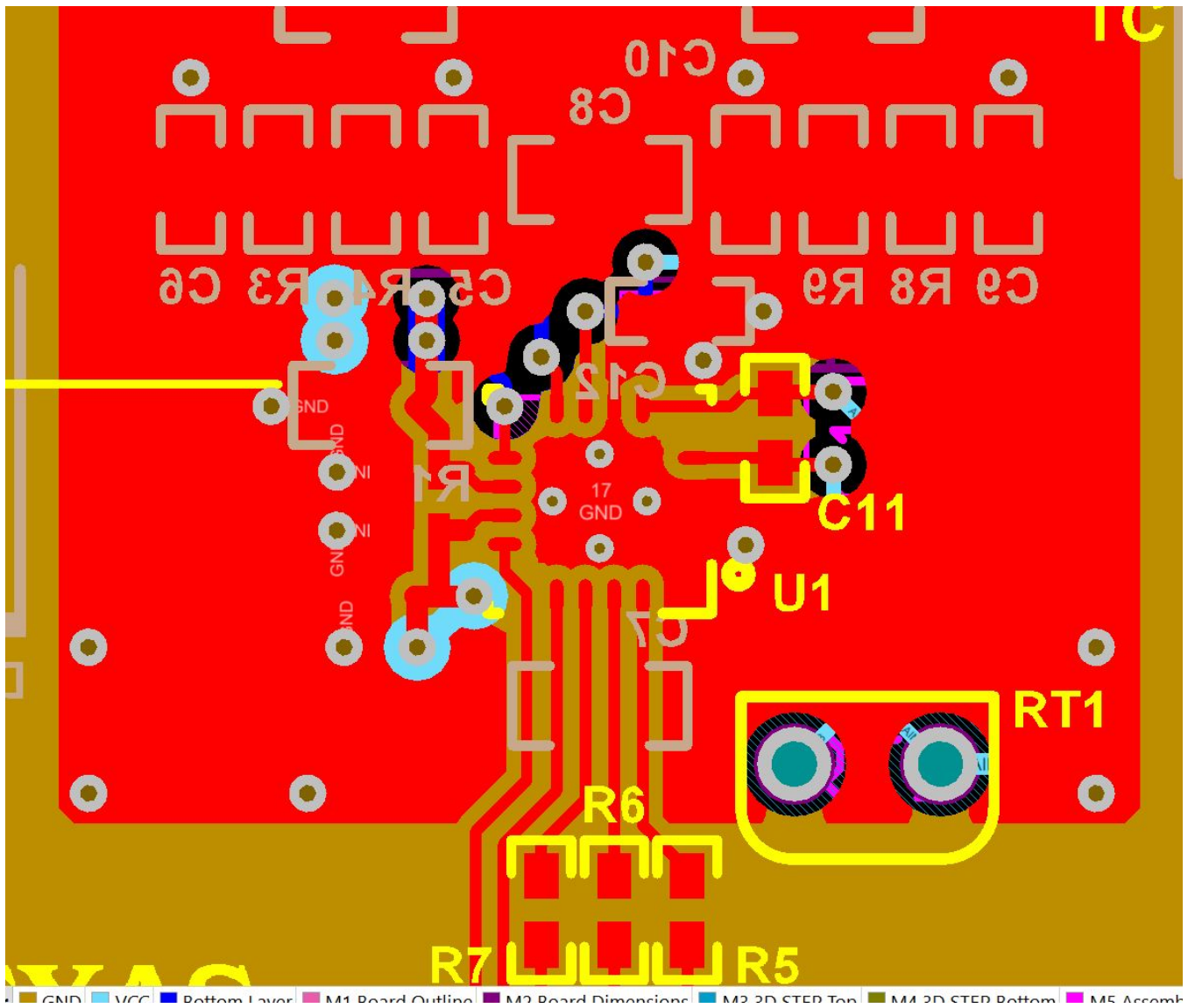


Figure 9. RTD Top Layer Placement

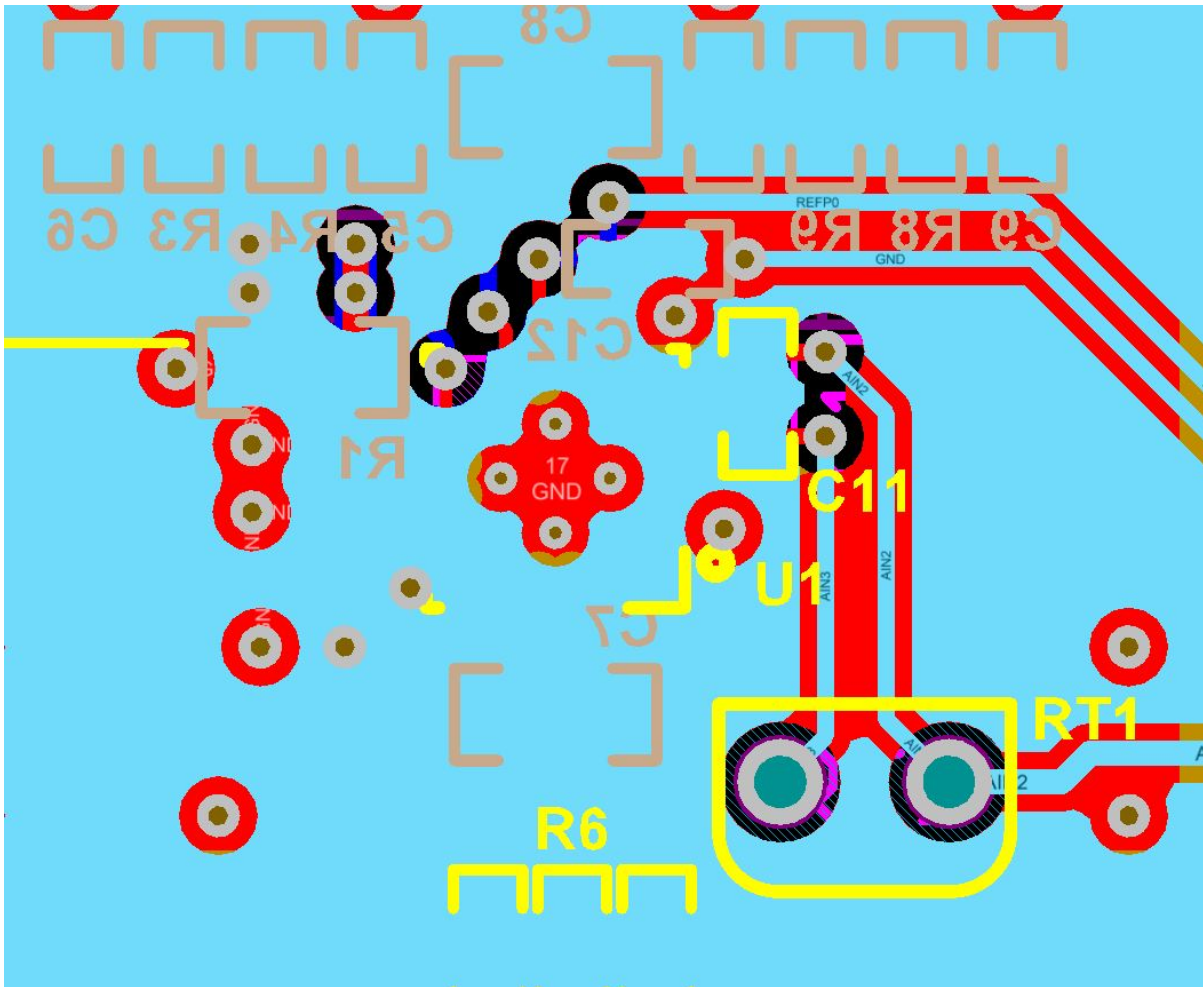
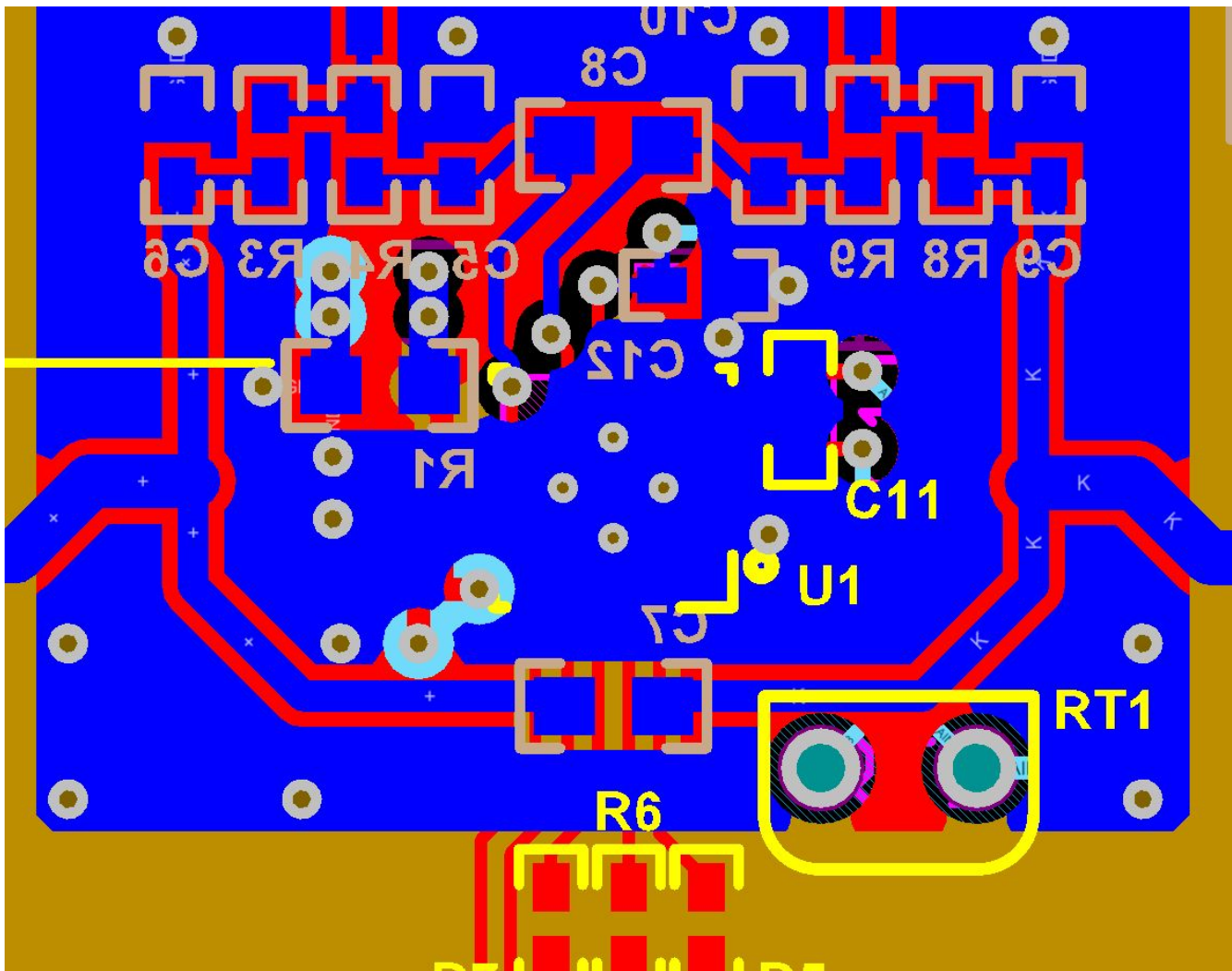


Figure 10. RTD Internal Layer Placement



**Figure 11. RTD Bottom Layer Placement**

As can be seen in [Figure 9](#) to [Figure 11](#), a lot of the components for the design must be squeezed into a small space, which complicates the routing and requires EMI and noise consideration. At the same time, the circuit designer may have to perform multiple iterations of the board development based on the simulation and actual results from testing, which increases the cost and time for the development of the field transmitter.

[Figure 12](#) shows the same component placement for the TMP117 in an isothermal block.

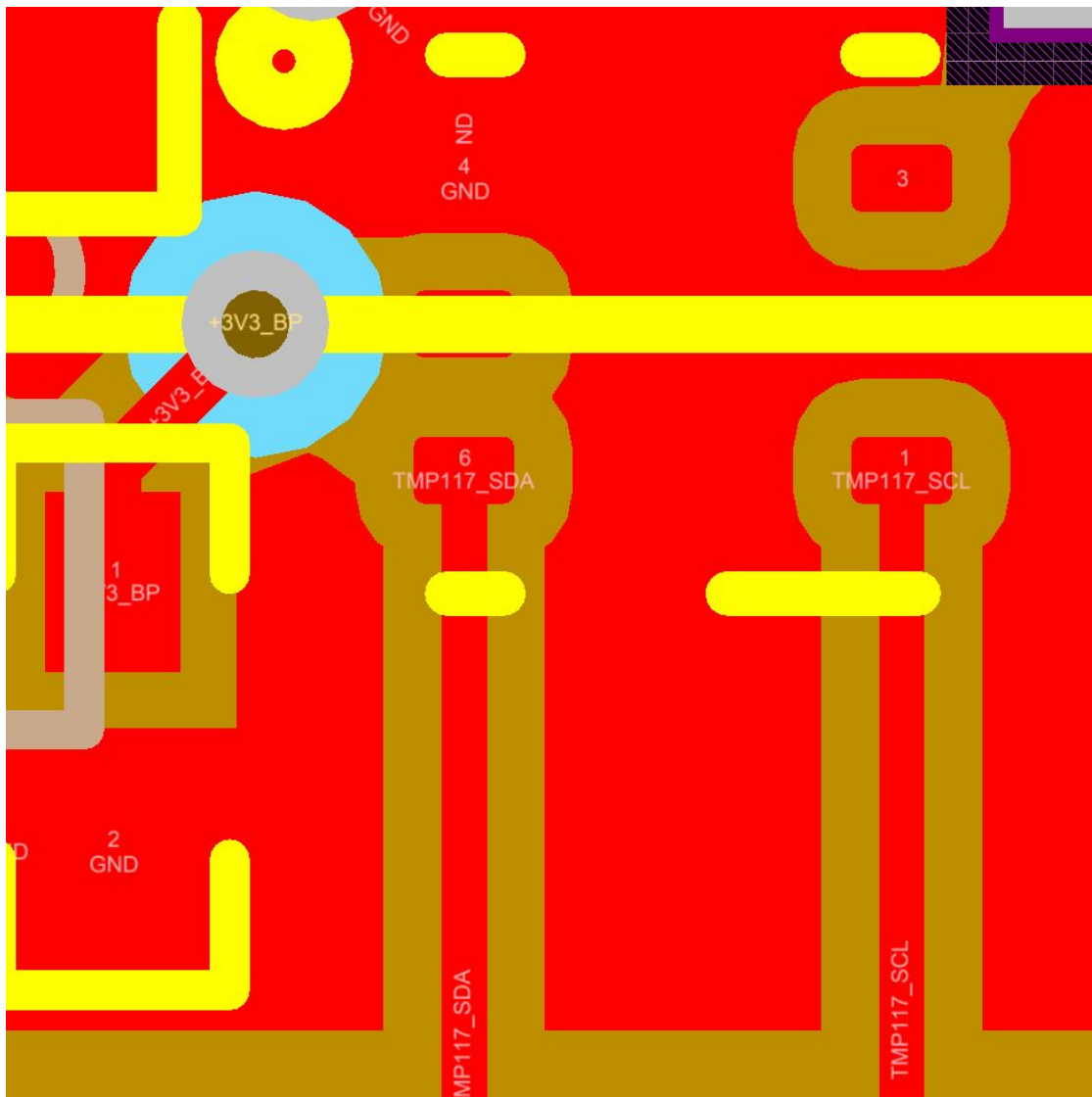
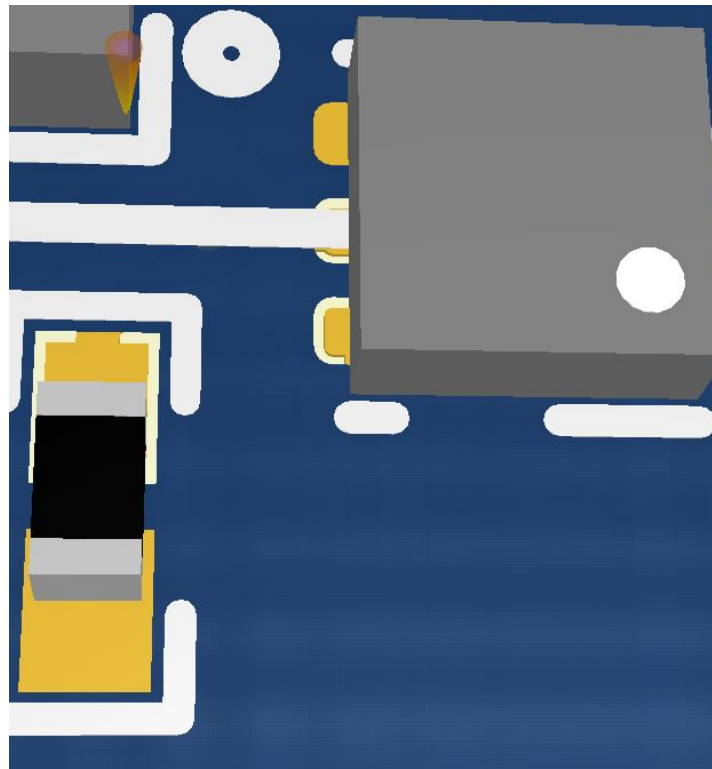


Figure 12. TMP117 Placement



**Figure 13. TMP117 3D Placement View**

Figure 13 shows a 3D model of the same placement. For reference, the end-to-end placement of the TMP117 and its decoupling capacitor is approximately 220 mils. The pullup resistors are not required in the thermally-critical area, thus reducing the complexity of the layout. As a digital temperature sensor, the communication noise may have a small effect on the temperature sensed by the TMP117. This saves a lot of time and redevelopment costs for the system designer.

### 2.3.4 Energy Consumption Analysis

The previous section highlighted the effect of an RTD on the cost of the system. This section highlights the effect an RTD-based system has on power consumption. A field transmitter may be battery-powered or line-powered. In the former case, it is necessary that the amount of energy consumed is as low as possible. The energy consumed by a circuit can be described by Equation 2.

$$\text{Energy} = \text{Voltage} \times \text{Current} \times \text{Time} \quad (2)$$

For further analysis, this example uses a precision ADC with the specifications for recommended operating conditions listed in Table 4. This ADC is a reference design for a temperature transmitter with an RTD element for CJC.

**Table 4. ADC Specification and Parameters**

Parameter Name	Parameter Description	Min	Typ	Max	Units
$I_{AVDD}^{1,2}$	Core supply current	–	235	300	$\mu\text{A}$
$I_{IOVDD}^1$	IO supply current	–	20	35	$\mu\text{A}$
$I_{AVDD-Increase}^1$	Independent of mode	–	19	25	$\mu\text{A}$
$I_{REF}^1$	Reference Current	–	250	–	$\mu\text{A}$
$F_{SAMP}^1$	Sampling Rate	–	25	–	SPS

- 
- NOTE:**
1. All parameters assume a supply voltage of 3.3 V.
  2. Gain of 16 for RTD measurement
- 

To solve the energy equation, the designer must calculate each part of the equation separately. As already established to improve the loss of accuracy arising due to current mismatch, the designer must perform the data acquisition twice. Hence, total active time for the RTD measurement can be calculated in [Equation 3](#):

$$\text{Time} = 2 \div F_{\text{SAMP}} \quad (3)$$

So, Time =  $2 \div 25 \text{ Hz} = 80 \text{ ms}$

The total current consumed during the active time is a sum of the current as given in [Table 4](#) and can be calculated in [Equation 4](#):

$$\text{Current} = I_{\text{AVDD}} + I_{\text{IOVDD}} + I_{\text{AVDD-Increase}} + 2 \times I_{\text{REF}} \quad (4)$$

So, Current =  $235 \mu\text{A} + 20 \mu\text{A} + 19 \mu\text{A} + 2 \times 250 \mu\text{A} = 774 \mu\text{A}$

The supply voltage is 3.3 V for both the core and the IO, therefore, this data can now be fed back into [Equation 2](#).

Energy =  $3.3 \text{ V} \times 774 \mu\text{A} \times 80 \text{ ms} = 204.336 \mu\text{J}$

The energy consumed by the ADC during RTD measurements shown here are for the typical condition, assuming that there is instantaneous communication between the MCU and the ADC. In real systems, this is a non-zero time parameter, along with the actual current consumption for the ADC, is based on the operating environment. Also, this does not take into account the current consumption by the MCU, which is waiting on the conversion result to perform CJC.

When the CJC system is based on the TMP117 to achieve  $\pm 0.1^\circ\text{C}$  accuracy, the operating conditions specified is for eight averages with a total active time of 125 ms. The quiescent current during an active measurement as per the TMP117 datasheet is  $135 \mu\text{A}$ . Solving [Equation 2](#) for TMP117 results in:

Energy =  $3.3 \text{ V} \times 135 \mu\text{A} \times 125 \text{ ms} = 55.6875 \mu\text{J}$ .

The energy savings is almost 73% for the TMP117 compared to the RTD-based temperature sensor. [Section 2.4](#) shows how this energy savings can have a more profound effect at a system level.

### 2.3.5 Self-Heating Analysis

A critical factor that engineers must take into account when designing a system with an RTD sensor is to calibrate the system for the effects of self-heating from the sensor. All three of the RTD constructions shown in this document require a constant current source to drive a known current through the RTD sensor to measure a voltage that is proportional to the resistance, and in turn is proportional to the temperature. If the constant current source is too small, then the voltage is too small by Ohm's law. Hence, TI recommends that the system designer increase the current flowing through the RTD sensor to make the measurements more accurate.

The effect that self heating, however, must also be factored into the overall accuracy. The temperature rise due to self heating is given by [Equation 5](#).

$$\Delta T = (I^2 \times R_{\text{RTD}}) \times \theta$$

where

- $\Delta T$  = the change in temperature due to self heating
  - $I$  = the excitation current
  - $R_{\text{RTD}}$  = the resistance of the RTD at the temperature of measurement
  - $\theta$  = the self heating coefficient in  $^\circ\text{C}/\text{mW}$
- (5)

As the excitation current is increased, the temperature rise due to self heating increases by a square factor. Also, with the changing RTD resistance, the effect of self-heating at higher temperatures of operation is more pronounced. There are techniques to compensate or reduce the effect of the drift error so introduced, which require either a full-scale calibration or specialized sigma-delta converters. In either case, the cost and complexity of the RTD-based compensation circuit increases.

On the contrary, with the TMP117, the average power is very small due to significant standby time between short temperature conversion time. This makes the self-heating effect negligible and simplifies the system designer's task, as they have one less effect to consider that impacts the accuracy of the design.

## 2.4 Software Analysis

The previous sections described the design considerations of RTD vs TMP117 that must be carefully understood and analyzed by a system designer. However, these considerations also manifest in terms of software development. In both system examples of RTD and TMP117-based CJC, the thermocouple output must be sampled by the AFE. As described in [Section 2.3.4](#), however, the RTD must be sampled twice to reduce the effect of the mismatch due to the current source on the RTD measurement. Taking the sampling rate of 25 SPS as mentioned in [Table 4](#), the software flow is graphically shown in [Figure 14](#).

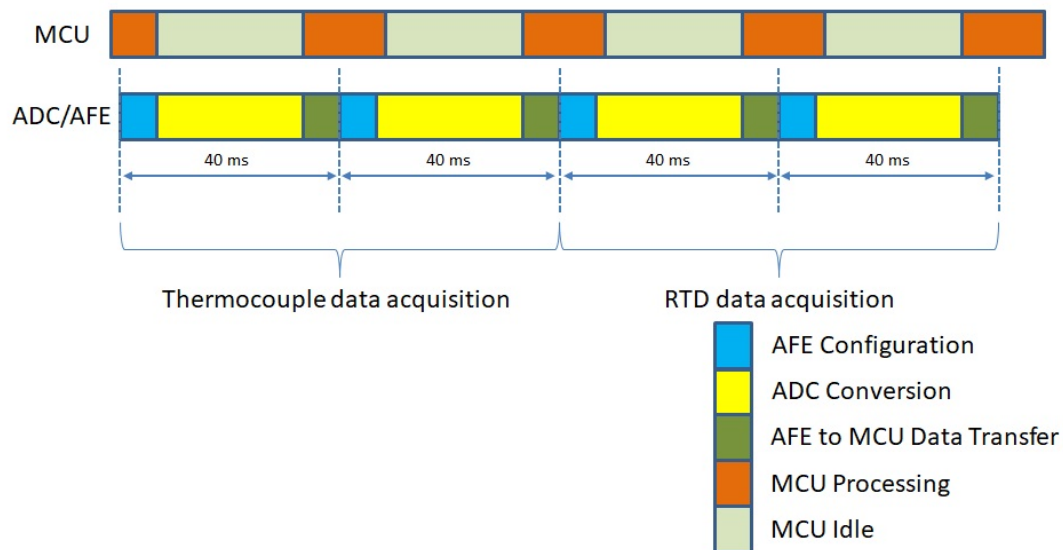


**Figure 14. RTD Software Time Graph**

As can be seen in time graph for RTD, the MCU must remain in idle time longer and also process the data from the AFE more times, thus resulting in higher energy consumption from a system perspective. However, this can be simplified with the TMP117 (see [Figure 15](#)).

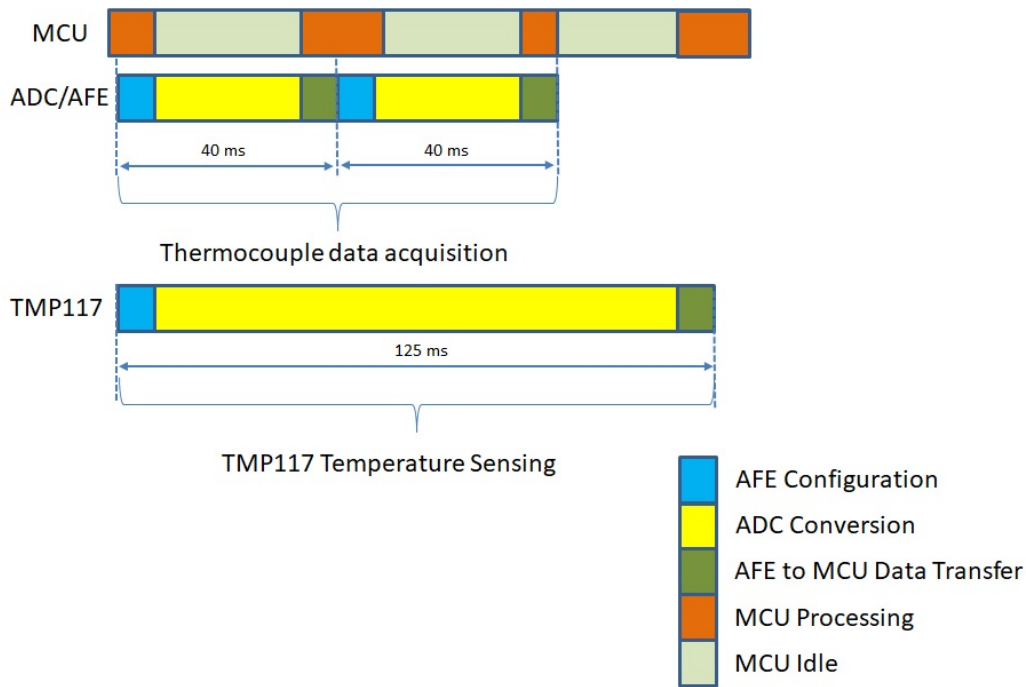


**Figure 15. TMP117 Software Time Graph**

As seen in the TMP117 software time graph, the TMP117 temperature sensing can be started in parallel to the thermocouple data acquisition. This allows the MCU to spend far less time in active and idle state, and more time in an ultra-low power state, thus reducing the overall system energy consumption. The actual value for the savings would vary from the choice of MCU selection, but is significant nonetheless.

### 3 Related Designs

[TIDA-010019](#) demonstrates design and evaluation of several different CJC blocks using a selection of analog and digital IC temperature sensors alongside an RTD solution. [Figure 16](#) shows the functional blocks of the design, which include the TMP117 (digital) and LMT70 (analog) ultra high accuracy temperature sensors, as well as the LMT01 (2-pin pulse) and the TMP235 (analog) temperature sensors to span the range of accuracy and features. For more information, the design guide and design files can be found at <http://www.ti.com/tool/TIDA-010019>.

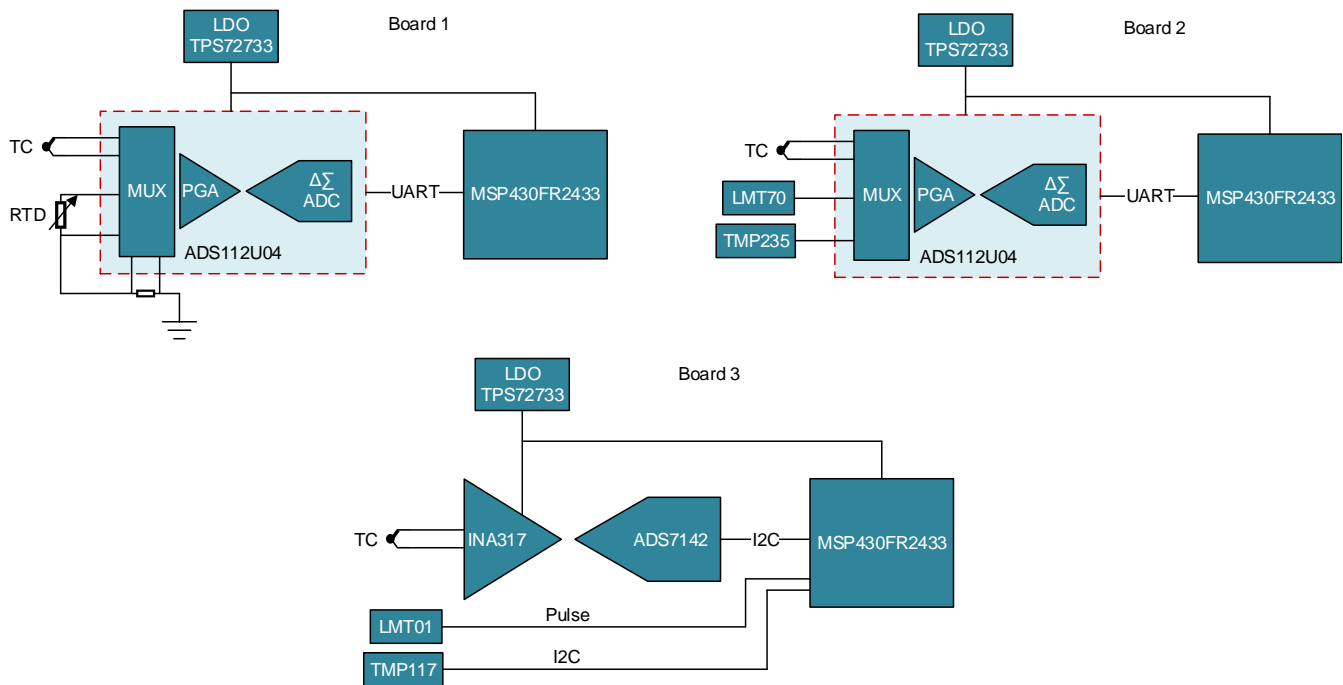


**Figure 16. TIDA-010019 Block Diagram**

## 4 Summary

This application report described two methods for CJC for temperature transmitters with the same level of accuracy. A system based on TMP117 high-precision temperature sensor helps reduce system design complexity, and lower system cost and development time compared to an RTD class-AA sensor. At the same time, the energy savings of at least 73% helps improve the overall life of temperature transmitter in field. The same method can be applied by system designers to other field transmitters where temperature compensation is required, and they can realize more simple and cost-effective systems without the need for extensive calibration with the TMP117.

## 5 References

The following related material have been used for the application report:

- [TMP117 ±0.1 °C Accurate Digital Temperature Sensor.](#)
- [Excitation Current Mismatch Effects in Three-wire RTD Measurement Systems.](#)
- [RTD Replacement for Cold Junction Compensation Reference Design in a Temperature Sensor \(TIDUEE1\)](#)

## Revision History

NOTE: Page numbers for previous revisions may differ from page numbers in the current version.

<b>Changes from Original (November 2018) to A Revision</b>	<b>Page</b>
• Edited application report for clarity. ....	1
• Updated <a href="#">Figure 1</a> .....	1
• Updated <a href="#">Figure 1</a> .....	2
• Updated <a href="#">Section 3</a> .....	19
• Added the reference design to <a href="#">Section 5</a> .....	20

## IMPORTANT NOTICE AND DISCLAIMER

TI PROVIDES TECHNICAL AND RELIABILITY DATA (INCLUDING DATASHEETS), DESIGN RESOURCES (INCLUDING REFERENCE DESIGNS), APPLICATION OR OTHER DESIGN ADVICE, WEB TOOLS, SAFETY INFORMATION, AND OTHER RESOURCES "AS IS" AND WITH ALL FAULTS, AND DISCLAIMS ALL WARRANTIES, EXPRESS AND IMPLIED, INCLUDING WITHOUT LIMITATION ANY IMPLIED WARRANTIES OF MERCHANTABILITY, FITNESS FOR A PARTICULAR PURPOSE OR NON-INFRINGEMENT OF THIRD PARTY INTELLECTUAL PROPERTY RIGHTS.

These resources are intended for skilled developers designing with TI products. You are solely responsible for (1) selecting the appropriate TI products for your application, (2) designing, validating and testing your application, and (3) ensuring your application meets applicable standards, and any other safety, security, or other requirements. These resources are subject to change without notice. TI grants you permission to use these resources only for development of an application that uses the TI products described in the resource. Other reproduction and display of these resources is prohibited. No license is granted to any other TI intellectual property right or to any third party intellectual property right. TI disclaims responsibility for, and you will fully indemnify TI and its representatives against, any claims, damages, costs, losses, and liabilities arising out of your use of these resources.

TI's products are provided subject to TI's Terms of Sale ([www.ti.com/legal/termsofsale.html](http://www.ti.com/legal/termsofsale.html)) or other applicable terms available either on [ti.com](http://ti.com) or provided in conjunction with such TI products. TI's provision of these resources does not expand or otherwise alter TI's applicable warranties or warranty disclaimers for TI products.

Mailing Address: Texas Instruments, Post Office Box 655303, Dallas, Texas 75265  
Copyright © 2019, Texas Instruments Incorporated